Journal of Applied Polymer Science

Crystallization, Melting Behavior, and Crystal Structure of Reactive, Intumescent, Flame-Retardant Polypropylene

Guixun Li, Shaokui Cao, Shijun Zheng, Wanjie Wang, Yanxia Cao, Jingwu Wang
School of Materials Science and Engineering, Zhengzhou University, Zhengzhou 450052, People's Republic of China
Correspondence to: G. Li (E-mail: liguixun@zzu.edu.cn)

ABSTRACT: Polypropylene (PP)/2-({9-[(4,6-diamino-1,3,5-triazin-2-yl) amino]-3,9-dioxido-2,4,8,10-tetraoxa-3,9-diphosphaspiro [5.5] undecan-3-yl} oxy) ethyl methacrylate (EADP) composites were prepared by the blending of PP with EADP as a new flame-retardant material. The nonisothermal crystallization and melting behaviors of composites were investigated with differential scanning calorimetry (DSC). Their crystal morphologies and structures were studied by polarized optical microscopy (POM) and X-ray diffraction (XRD), respectively. The DSC results show that the addition of EADP increased the crystallization onset temperature, crystallization peak temperature, and degree of crystallinity of PP in the PP/EADP composites. The melting onset temperature and melting end temperature of the PP/EADP composites decreased slightly, whereas the melting peak temperature of the PP/EADP composites increased. The POM results show that the addition of EADP greatly reduced the crystal size of PP in the composites. When the content of EADP in the PP/EADP composites was increased, the crystal size of PP became smaller. The XRD results indicate that the addition of EADP changed the crystal structure of PP in the PP/EADP composites, which exhibited both α-form and β-form crystal structures.
 J. Appl. Polym. Sci. **2015**, *132*, 41374.

KEYWORDS: crystallization; flame retardance; morphology; polyolefins

Received 4 April 2014; accepted 1 August 2014
DOI: 10.1002/app.41374

INTRODUCTION

Polypropylene (PP) is used in a wide variety of applications because of its nontoxicity, easy processing, good chemical resistance, and excellent mechanical properties. It is particularly important to improve its flame retardancy because its easy flammability. Intumescent flame retardants (IFRs) have gradually been focused on because of their advantages, such as low smoke, nontoxicity, and lack of corrosive gas release during burning.[1,2] However, IFRs have some deficiencies,[3,4] including a lower thermal stability, lower water resistance, and poor compatibility with PP; this leads to a decrease in the flame retardancy and mechanical properties of PP.[5–7] The determination of a method for preparing a kind of IFR bearing good compatibility with PP, showing excellent flame retardancy, and maintaining mechanical properties of PP has become an important subject in research into environmentally friendly flame retardants.[8]

In our previous work, a reactive intumescent halogen-free flame-retardant, 2-({9-[(4,6-diamino-1,3,5-triazin-2-yl) amino]-3,9-dioxido-2,4,8,10-tetraoxa-3,9-diphosphaspiro [5.5] undecan-3-yl} oxy) ethyl methacrylate (EADP), which combines an acid source, a blowing agent, and a char-forming agent within one single molecule, was synthesized to prepare a flame-retardant PP. Composites of PP with EADP (PP/EADP) were prepared through reactive blending. A detailed investigation showed that the PP/EADP composites had good mechanical properties and outstanding flame retardancy.[9,10] It is well known that the nonisothermal crystallization, melting behavior, and crystal structure of polymer materials are closely related to their molding processes and mechanical properties.[11–16] For example, under practical conditions, PP tends to crystallize into β-form crystals; these show a better elongation at break, lower density, higher impact strength, and so on. Therefore, studies on the crystallization behavior and morphology of PP composites are very significant in both theory and practice.[17,18] In this study, the effect of EADP on the nonisothermal crystallization, melting behavior, and crystal structure of PP/EADP composites were investigated in detail.

EXPERIMENTAL

Materials

PP (F401), with a melt flow index of 2.3 g/10 min (230°C/2.16 kg), was obtained commercially from Luoyang Petrochemical Co., Ltd. EADP was synthesized according to a procedure in the literature,[9] and its chemical structure is shown in Figure 1. A commercial ammonium polyphosphate coated by melamine resin (MAPP), with an average degree of polymerization greater

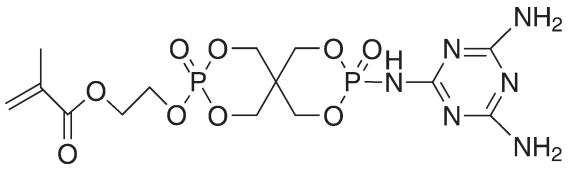

Figure 1. Molecular structure of EADP.

than 1000 and purchased from Puyang Chengke Chemical Technology Co., was used for comparison.

Preparation of the PP/EADP Composites

The PP/EADP composites were prepared with reactive blending in a high-speed mixer and then extruded with a twin-screw extruder (SHJ-20, Nanjing Giant Machinery Co., Ltd.) with a temperature profile of 175, 185, 195, 205, and 195°C. The composites were prepared from PP and EADP with compositions of 80/20, 75/25, 70/30, and 65/35 for samples of PP/EADP-20, PP/EADP-25, PP/EADP-30, and PP/EADP-35, respectively.

PP/MAPP-30 as a reference sample was prepared with a PP/MAPP ratio of 70/30 under the same conditions as those used for the PP/EADP composites.

Nonisothermal Crystallization and Melting Behavior

Differential scanning calorimetry (DSC) measurements were performed on a differential scanning calorimeter (DSC 204 Phoenix, Netzsch Co., Germany). Samples of about 5–10 mg were heated from 50 to 230°C at a heating rate of 10°C/min in a nitrogen atmosphere. When the temperature reached 230°C, the samples were maintained for 3 min and then cooled at a rate of 10°C/min. The crystallization exotherm and subsequent melting curves of the samples were recorded.

Crystal Morphology

PP and the PP/EADP and PP/MAPP-30 composites were placed between two cover glasses on a heating stage and heated to 230°C for 5 min. After 10 s of pressing, the samples were cooled down to 140°C at a cooling rate of 2.3°C/min and maintained at that temperature for 30 min. The crystal morphologies of the neat PP and its composites were recorded with a polarized optical microscope (Leica-DMLP, Leica, Germany).

Crystal structure

The samples were prepared on a thermal platform under primary experimental conditions. The X-ray diffraction (XRD) patterns of the samples were recorded on an X-ray diffractometer (D8 Advance X, Bruker Corp., Germany) at a voltage of 40 kV and a current of 40 mA with a scan step of 2°/min in the range $2\theta = 5–40°$.

RESULTS AND DISCUSSION

Effect of EADP on the Nonisothermal Crystallization Behavior of PP

Figure 2 shows the nonisothermal crystallization curves of PP and the PP/EADP and PP/MAPP-30 composites. Their crystallization parameters are listed in Table I. We observed that the values of the crystallization onset temperature (T_{co}), crystallization peak temperature (T_{cp}), and slope at the high-temperature side of the exothermic peak (S_i) of the PP/EADP and PP/MAPP-30 composites were higher than those of neat PP.

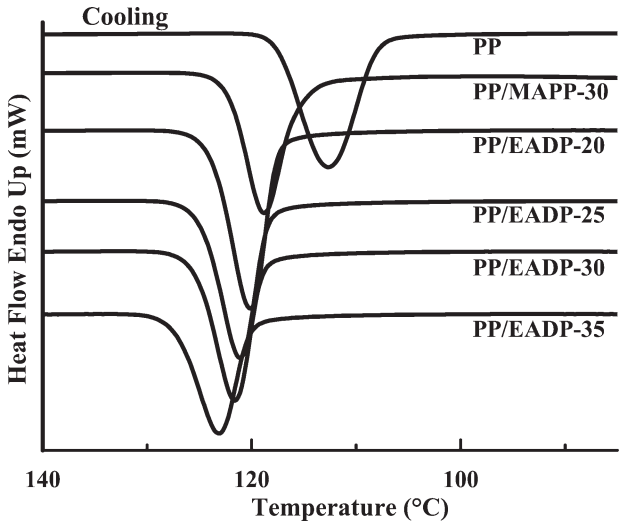

Figure 2. Nonisothermal crystallization curves of PP and the PP/EADP and PP/MAPP-30 composites.

For example, the T_{co} and T_{cp} values of the PP/EADP-30 composite increased by 7.73 and 9.00°C compared with those of neat PP because EADP and MAPP could both act as nucleating centers to reduce the undercooling and increase the rate of crystallization.[19–21] Furthermore, the T_{co} and T_{cp} values of the PP/EADP-30 composite were higher than those of PP/MAPP-30 by 4.86 and 4.57°C, respectively; this indicated that EADP was more beneficial for heterogeneous nucleation. Because a considerable number of EADP could be bonded to the PP chains during reactive blending and afford good compatibility between PP and EADP,[9] this reduced the free energy of the nucleation process and increased the rate of crystallization.[22,23]

The values of the width at half-height of the crystallization peak ($W_{1/2}$) of the PP/EADP and PP/MAPP-30 composites were smaller than that of neat PP; this indicated that the crystal size distributions of PP in the PP/EADP and PP/MAPP-30 composites were smaller than that of neat PP.[19,24]

The degree of crystallinity (X_c) values of PP and the PP/EADP and PP/MAPP-30 composites were calculated according to eq. (1), and the results are listed in Table I. The X_c values of PP in the PP/EADP and PP/MAPP-30 composites were higher than that of neat PP. There were two reasons for the increase in X_c. First, EADP and MAPP could act as heterogeneous nuclei and

Table I. DSC Results for PP and the PP/EADP and PP/MAPP Composites by Crystallization

Sample	T_{co} (°C)	T_{cp} (°C)	$W_{1/2}$ (°C)	S_i	X_c (%)
PP	117.63	112.60	5.81	2.35	40.97
PP/EADP-20	123.92	120.07	3.74	3.60	49.61
PP/EADP-25	124.90	121.09	3.74	3.83	52.48
PP/EADP-30	125.36	121.60	3.75	3.61	50.67
PP/EADP-35	127.30	123.06	4.23	3.06	47.37
PP/MAPP-30	120.50	117.03	4.04	2.80	48.95

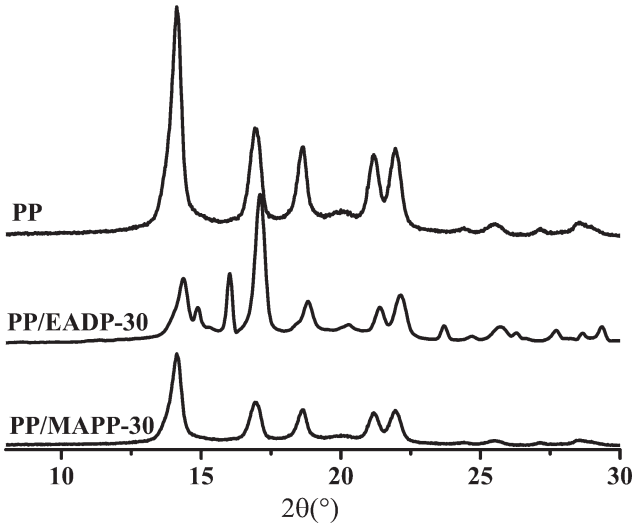

Figure 3. XRD curves of PP and the PP/EADP-30 and PP/MAPP-30 composites.

increase the number of crystal nuclei and improve the rate of crystallization. Second, PP in the PP/EADP and PP/MAPP-30 composites was crystallized at higher temperatures with enough thermal energy to allow more chain segments of PP to enter the lattice of the crystal.[19] Furthermore, we also found that the X_c of PP/EADP-30 was higher than that of PP/MAPP-30 because of the better compatibility of EADP with PP. The improved compatibility resulted in the crystallization temperature shifting to higher temperatures and an increase in the rate of crystallization to one faster than that of PP/MAPP-30; these were more beneficial for increasing the X_c of PP in the PP/EADP-30 composite.[25] Previous results indicate that the addition of EADP could increase the rate of crystallization, so the molding cycle of the PP/EADP composites were shortened compared with those of the neat PP and PP/MAPP-30 composite:

$$X_c = \frac{\Delta H_m}{\Delta H_m^0} \times 100\% \quad (1)$$

where ΔH_m is the enthalpy of fusion of PP or PP in PP/EADP and PP/MAPP-30 composites and $\Delta H_m{}^0$ is the enthalpy of 100% crystallized PP (209 J/g).[26]

The results also show that the addition of EADP had an obvious effect on the nonisothermal crystallization behaviors of the PP/EADP composites, as shown in Figure 2 and Table I. PP in PP/EADP-25 had the fastest rate of crystallization, the highest X_c, and the lowest crystal size distribution. This was caused by two opposite effects of EADP on the nonisothermal crystallization behavior of PP. On the one hand, the compatibility of EADP with PP was enhanced, with a considerable number of EADP bonded into the PP molecule chain; this improved the disperision of EADP and the heterogeneous nucleation effect. Then, the free energy of PP crystallization decreased. The temperature and rate of crystallization of PP increased;[19] this caused X_c to increase. On the other hand, the addition of EADP hindered the PP segmental rearrangement to the surface of the crystal nucleus and into the cyrstal lattice. In particular, with the increased content of EADP, this inhibition effect was evident, such as when the content of EADP reached 35 wt %. So, the rate of crystallization and X_c of PP in PP/EADP-35 were lower than those in PP/EADP-25, and the crystal size distribution of PP in PP/EADP-35 was higher than that of PP/EADP-25.

Effect of EADP on the Crystal Structure of PP

The XRD curves of PP and the PP/EADP-30 and PP/MAPP-30 composites are shown in Figure 3. Neat PP was crystallized in α-form crystal; this resulted from the presence of the reflections at $2\theta = 14.06$, 16.92, 18.64, 21.18, and 21.94°, which corresponded to 110, 040, 130, 111, and 131 diffractions, respectively.[27–30] There was an extra reflection at a 2θ of 15.94° in the curve of PP/EADP-30, which belonged to the (300) lattice planes of the β-form crystal of PP.[30–33] The results indicate that the addition of EADP induced PP to form β-form crystals, although two kinds of crystal structure coexisted in the PP/EADP-30 composite. The relative content of the β phase (k_β) was calculated as 0.24 according to eq. (2).[32,34] The curve of PP/MAPP-30 was the same as that of neat PP; this suggested that MAPP had no effect on the crystal structure of PP:[35]

$$k_\beta = \frac{H_\beta(300)}{H_\beta(300) + H_\alpha(110) + H_\alpha(040) + H_\alpha(130)} \quad (2)$$

where $H_\beta(300)$ is the diffraction intensity of the β(300) planes and $H_\alpha(110)$, $H_\alpha(040)$, and $H_\alpha(130)$ are the diffraction intensities of the α(110), α(040), and α(130) planes, respectively.

Effect of EADP on the Crystal Morphology of PP

Polarized optical microscopy (POM) images of PP, PP/EADP and PP/MAPP-30 composites are presented, respectively in Figure 4. Neat PP shows a typical morphology of spherulites and the crystal size is obviously bigger than those of PP/EADP and PP/MAPP-30 composites. The results indicate that EADP and MAPP could act as heterogeneous nuclei and increase both the number of crystal nuclei and the rate of crystallization. With the content increase of EADP, the crystal size of PP in composites became smaller.

Effect of EADP on the Melting Behavior of PP

The melting curves of PP and the PP/EADP and PP/MAPP-30 composites are shown in Figure 5. The melting onset temperature (T_{mo}), melting peak temperature (T_{mp}), melting end temperature (T_{me}), and ΔH_m are listed in Table II. The T_{mo} and T_{me} values of the PP/EADP composites were slightly lower than those of neat PP. There were three factors constraining the melting behavior of PP: the crystal structure, maximum regular degree of crystal structure, and dispersion of the regular degree of crystal structure. In general, the value of T_{mo} of PP/EADP was obviously lower than that of neat PP because the melting temperature of the β-form crystal for PP was evidently lower than that of the α-form crystal.[36] However, in our case, EADP as a heterogeneous nuclei increased the temperature of crystallization by decreasing the free energy of PP cystallization. As a result, the maximum regular degree of crystal structure was increased, and the dispersion of the regular degree of crystal structure was decreased. In addition, the content of β-form crystal was small, and some β-form crystals could change to α-form crystals during the heating process;[37,38] this resulted in the T_{mo} values of the PP/EADP composites decreasing slightly. The

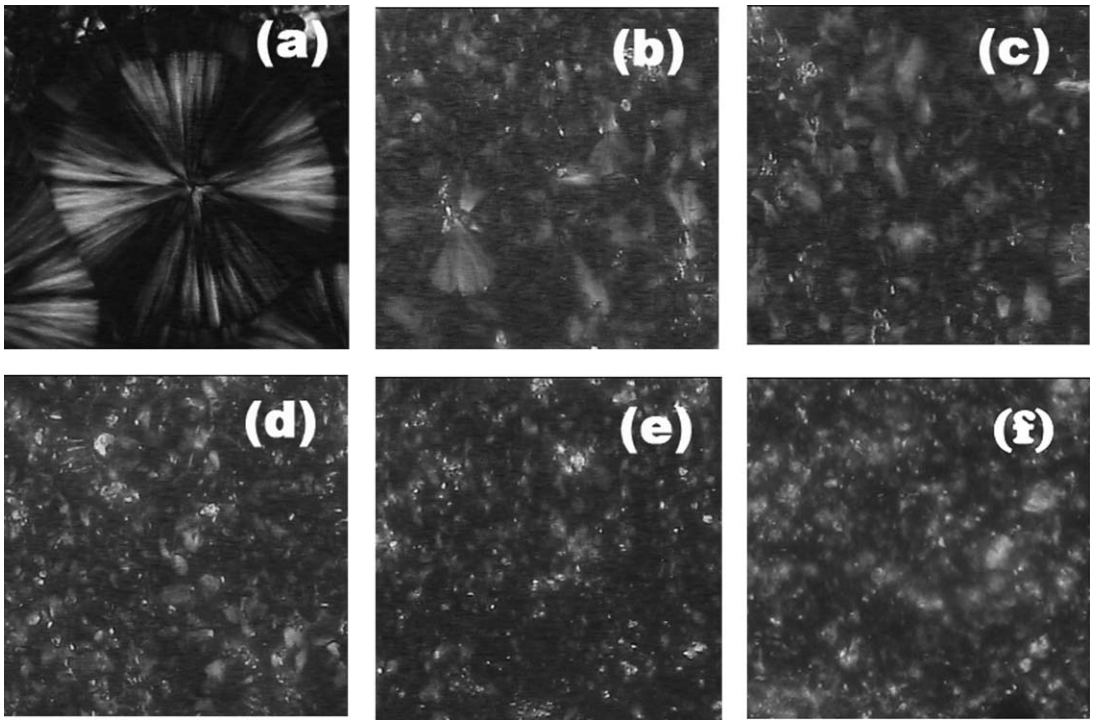

Figure 4. POM photographs of PP and the PP/EADP and PP/MAPP-30 composites (500×): (a) PP, (b) PP/EADP-20, (c) PP/EADP-25, (d) PP/EADP-30, (e) PP/EADP-35, and (f) PP/MAPP-30.

T_{mp} values of the PP/EADP composites increased; this was directly related to the dispersion of the regular degree of PP crystal structure. When EADP was added into PP, the dispersion of the regular degree of PP crystal structure decreased, and the crystal size of PP was more uniform; this led to an increase in the T_{mp} values.

The crystal structure of PP in the PP/MAPP-30 composite was the same as that of the neat PP, whereas the T_{mo} and T_{mp} values of PP/MAPP-30 were lower than those of the neat PP. Despite the T_{co}, T_{cp}, and S_i values of PP/MAPP-30 were higher than those of neat PP, the variation range of those values of PP/MAPP-30 was less than that of PP/EADP-30. The result indicates that the compatibility between MAPP and PP was not as good as that between EADP and PP.[22] Moreover, MAPP hindered the rearrangement of PP segment into the lattice. All of those effects led to a slight increase in the rate of crystalization and a decrease in the crystalline regularity of PP in the PP/MAPP-30 composites.

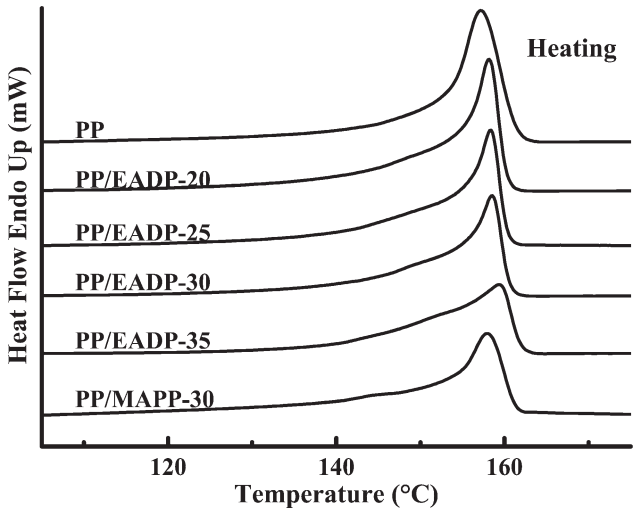

Figure 5. Melting curves of PP and the PP/EADP and PP/MAPP-30 composites.

In summary, compared with neat PP, the addition of EADP increased X_c and decreased the crystal size of PP in the composites; this made a number of connecting chains between the crystalline and amorphous regions and increased the interphase force.[39] Furthermore, EADP had good compatibility with PP, and this resulted in a uniform distribution of EADP and enhanced the interfacial adhesion between EADP and PP in the PP/EADP composites. On the basis of those structural features, the PP/EADP composites had good static mechanical properties

Table II. DSC Results for PP and the PP/EADP and PP/MAPP Composites by Melting

Sample	T_{mo} (°C)	T_{mp} (°C)	T_{me} (°C)	ΔH_m (J/g)[a]
PP	152.63	157.13	161.37	85.62
PP/EADP-20	151.90	158.18	160.23	103.68
PP/EADP-25	150.28	158.20	160.53	109.69
PP/EADP-30	150.02	158.56	160.56	103.40
PP/EADP-35	149.53	158.77	160.88	99.00
PP/MAPP-30	149.65	156.19	160.84	101.31

[a] ΔH_m of PP or PP in the PP/EADP and PP/MAPP-30 composites.

compared to those of neat PP. In particular, β-form crystals, which have the potential to improve the impact toughness, were formed in the PP/EADP composites.[20] As a result, the PP/EADP composites not only had excellent flame-retardant properties but also presented good comprehensive mechanical properties.[9,10]

CONCLUSIONS

PP/EADP composites were prepared with reactive blending and characterized by DSC, XRD, and POM. The results indicate that the values of T_{co}, T_{cp}, S_i, and X_c of PP in the PP/EADP composites were higher than those of neat PP. The PP/EADP-25 composite had the fastest crystallization rate and the highest X_c. The T_{mo} and T_{me} values of PP in the PP/EADP composite decreased slightly compared with the neat PP, whereas the T_{mp} value increased a little. For example, the T_{co} and T_{cp} values of PP in the PP/EADP-30 composite with 30 wt % EADP increased about 7.73 and 9.00°C, respectively. The PP X_c in PP/EADP-30 increased about 9.70% compared with that of neat PP. The POM results show that the crystal size of PP in the PP/EADP composites lowered obviously compared with that of neat PP. The larger content of EADP induced the smaller crystal size of PP. The XRD results show that PP in the PP/EADP composites had both α-form and β-form crystal structures.

REFERENCES

1. Feng, C.; Zhang, Y.; Liu, S. W.; Chi, Z. G.; Xu, J. R. *J. Appl. Polym. Sci.* **2012**, *123*, 3208.
2. Yang, X.; Ge, N.; Hu, L.; Gui, H.; Wang, Z.; Ding, Y. *Polym. Adv. Technol.* **2013**, *24*, 568.
3. Zhou, J.; Yang, L.; Wang, X. L.; Fu, Q. J.; Sun, Q. L.; Zhang, Z. Y. *J. Appl. Polym. Sci.* **2013**, *129*, 36.
4. Wu, K.; Shen, M.-M.; Hu, Y. *J. Polym. Res.* **2011**, *18*, 425.
5. Yi, J. S.; Yin, H. Q.; Cai, X. F. *J. Therm. Anal. Calorim.* **2013**, *111*, 725.
6. Yi, J.; Liu, Y.; Pan, D.; Cai, X. *J. Appl. Polym. Sci.* **2013**, *127*, 1061.
7. Yang, K.; Xu, M. J.; Li, B. *Polym. Degrad. Stab.* **2013**, *98*, 1397.
8. Wang, N.; Zhang, J.; Fang, Q. H.; Hui, D. *Compos. B* **2013**, *44*, 467.
9. Li, G. X.; Wang, W. J.; Cao, S. K.; Cao, Y. X.; Wang, J. W. *J. Appl. Polym. Sci.* **2014**, *131*, 3314.
10. Li, G. X.; Cao, S. K.; Wang, W. J.; Cao, Y. X.; Wang, J. W. *Polym. Mater. Sci. Eng.* **2014**, *30*, 72.
11. Chu, W. Y.; Tai, H. J.; Chen, L. W.; Chu, L. H. *J. Appl. Polym. Sci.* **1991**, *43*, 521.
12. Qin, J.; Li, Z. *J. Appl. Polym. Sci.* **2010**, *115*, 1256.
13. Qin, J.; Guo, S.; Li, Z. *J. Appl. Polym. Sci.* **2008**, *109*, 1515.
14. Lin, Z.; Qiu, Y.; Mai, K. *J. Appl. Polym. Sci.* **2004**, *92*, 3610.
15. Cui, L.; Zhang, Y.; Zhang, Y. *J. Polym. Sci. Part B: Polym. Phys.* **2006**, *44*, 3288.
16. Saujanya, C.; Radhakrishnan, S. *Polymer* **2001**, *42*, 6723.
17. Wang, S.; Zhang, J.; Chen, S.; Zhu, H. *J. Cryst. Growth* **2012**, *355*, 151.
18. Wang, J.; Dou, Q. *Polym. Int.* **2008**, *57*, 233.
19. Gupta, A. K.; Purwar, S. N. *J. Appl. Polym. Sci.* **1984**, *29*, 1595.
20. Zhang, R. Y.; Ma, D. Z.; Luo, X. L. *Polym. Mater. Sci. Eng.* **1991**, *7*, 55.
21. He, M. J.; Chen, W. X.; Dong, X. X. Polymer Physics; Fudan University Press: Shanghai, **1990**.
22. Lu, M. F.; Zhang, S. J.; Yu, D. S. *J. Appl. Polym. Sci.* **2004**, *93*, 412.
23. Lin, Z.; Chen, C.; Li, B.; Guan, Z.; Huang, Z.; Zhang, M.; Li, X.; Zhang, X. *J. Appl. Polym. Sci.* **2012**, *125*, 1616.
24. Li, Y.; Xu, J.-T.; Dong, Q.; Wang, X.-P.; Fu, Z.-S.; Fan, Z.-Q. *Polym. Plast. Technol. Eng.* **2008**, *47*, 1242.
25. Wang, B.; Hu, G.; Wei, L. *J. Appl. Polym. Sci.* **2008**, *107*, 3013.
26. Wunderlich, B. Thermal Analysis; Academic: Salt Lake City, UT, **1990**.
27. Zhang, L.; Yang, M. Z.; Shi, G.; Zhang, C. *Polym. Mater. Sci. Eng.* **2010**, *26*, 78.
28. Cui, L.; Wang, S.; Zhang, Y.; Zhang, Y. *J. Appl. Polym. Sci.* **2007**, *105*, 379.
29. Chen, X. L.; Yu, J.; Guo, S. Y.; Luo, Z.; He, M. *Polym. Compos.* **2009**, *30*, 941.
30. Li, S. C.; Liu, H.; Zeng, W. *J. Appl. Polym. Sci.* **2011**, *121*, 2614.
31. Papageorgiou, D. G.; Papageorgiou, G. Z.; Bikiaris, D. N.; Chrissafis, K. *Eur. Polym. J.* **2013**, *49*, 1577.
32. Mo, Z. S.; Zhang, H. F. Crystalline Polymer Structure and X-Ray Diffraction; Science: Beijing, **2003**.
33. Minardi, A.; Boudeulle, M.; Duval, E.; Etienne, S. *Polymer* **1997**, *38*, 3957.
34. Zhang, Z. S.; Tao, Y. J.; Yang, Z. G.; Mai, K. C. *Eur. Polym. J.* **2008**, *44*, 1955.
35. Vuillequez, A.; Lebrun, M.; Ion, R. M.; Youssef, B. *Macromol. Symp.* **2010**, *290*, 146.
36. Grein, C.; Plummer, C. J. G.; Kausch, H. H.; Germain, Y.; Béguelin, P. *Polymer* **2002**, *43*, 3279.
37. Wunderlich, B. Macromolecular Physics; Academic: New York, **1973**.
38. Shangguan, Y.; Song, Y.; Peng, M.; Li, B.; Zheng, Q. *Eur. Polym. J.* **2005**, *41*, 1766.
39. Wang, J. W. Plastic Modification Technology; Chemical Industry: Beijing, **2004**.